Detecting cell-adhesive sites in extracellular matrix using force spectroscopy mapping

Detecting cell-adhesive sites in extracellular matrix using force spectroscopy mapping

Somyot Chirasatitsin and Adam J Engler[1]

Department of Bioengineering, University of California, San Diego, 9500 Gilman Drive,
MC 0412, La Jolla, CA 92093, USA

E-mail: aengler@ucsd.edu

Abstract
The cell microenvironment is composed of extracellular matrix (ECM), which contains specific binding sites that allow the cell to adhere to its surroundings. Cells employ focal adhesion proteins, which must be able to resist a variety of forces to bind to ECM. Current techniques for detecting the spatial arrangement of these adhesions, however, have limited resolution and those that detect adhesive forces lack sufficient spatial characterization or resolution. Using a unique application of force spectroscopy, we demonstrate here the ability to determine local changes in the adhesive property of a fibronectin substrate down to the resolution of the fibronectin antibody-functionalized tip diameter, ~20 nm. To verify the detection capabilities of force spectroscopy mapping (FSM), changes in loading rate and temperature were used to alter the bond dynamics and change the adhesion force. Microcontact printing was also used to pattern fluorescein isothiocyanate-conjugated fibronectin in order to mimic the discontinuous adhesion domains of native ECM. Fluorescent detection was used to identify the pattern while FSM was used to map cell adhesion sites in registry with the initial fluorescent image. The results show that FSM can be used to detect the adhesion domains at high resolution and may subsequently be applied to native ECM with randomly distributed cell adhesion sites.

S Online supplementary data available from stacks.iop.org/JPhysCM/22/194102/mmedia

(Some figures in this article are in colour only in the electronic version)

1. Introduction

Adhesion to the surrounding environment is an important cell behavior that regulates a variety of processes, e.g. motility (Chien *et al* 2005, Li *et al* 2005), matrix remodeling (Hinz and Gabbiani 2003, Sharma *et al* 2008), cancer metastasis (Ingber 2008, Kumar and Weaver 2009) and even signaling and gene expression (Chiquet *et al* 2009, Engler *et al* 2009b). As the cell starts to attach to its environment, which is composed of a large fibrillar network of proteins known as extracellular matrix (ECM), it does so by forming clusters of proteins that bind to ECM, known as focal adhesions; these adhesions connect the cell's cytoskeleton to ECM and enable the cell to contract against it. Yet given its fibrillar nature

and localization in tissues, the distribution of ECM *in vivo* is not uniform (Hay 1991). Moreover, ECM proteins contain only a few small adhesive sites and cell binding can occur only at these sites, e.g. the R–G–D peptide sequence on the 10th type 3 domain of fibronectin binds to $\alpha_5\beta_1$ integrins in focal adhesions (Ruoslahti and Pierschbacher 1987). With such specificity and a limited number of sites of adhesion with ECM, characterization of receptor–ligand interactions and their distribution in a natural or synthetic material must be equally specific for accurate control of cell behavior to be possible. Moreover, these interactions are mechanical in nature as they link force-generating proteins, e.g. myosin, to ECM. Adhesion mechanisms are especially important given that force-dependent integrin behavior regulates the activity of many proteins, e.g. Rho GTPases, resulting in changes in cell behavior and phenotype (Puklin-Faucher and Sheetz 2009);

---

[1] Author to whom any correspondence should be addressed.

thus measurement methods that determine the force that cell adhesions can withstand would provide an additional mode for evaluating cell adhesion.

Many techniques have been used to investigate the mechanical properties of receptor–ligand interactions, both population-based (Engler *et al* 2009a) and single-cell-based ones (Shao *et al* 2004), and have been performed using native (Engler *et al* 2009a) and synthetic environments (Griffin *et al* 2004). Spinning disc assays, as population-based measures, apply a uniform or radially dependent shear profile that can examine the detachment force of a group of cells, and they have been used to demonstrate the importance of matrix dimensionality (Engler *et al* 2009a), focal adhesion clustering (Gallant *et al* 2005), and adhesive domain conformation (Friedland *et al* 2009). On the other hand, single-cell techniques such as micropipette aspiration (Griffin *et al* 2004, Shao *et al* 2004), force spectroscopy (Dufrene and Hinterdorfer 2008, Ludwig *et al* 2008), and optical tweezers (Jiang *et al* 2003) are very sensitive and can measure the tens of piconewtons required to rupture single integrin–ECM bonds (Jiang *et al* 2003, Sun *et al* 2005). For force spectroscopy, a probe is functionalized with receptors or oppositely charged macromolecules (Florin *et al* 1994), making it stick to ligands immobilized on a substrate. As the probe translates up from the substrate, the bond tenses until it ruptures, and this force is then determined from plots of probe force versus position relative to the substrate's surface (Muller *et al* 2009). While accurately measuring forces, none of these techniques provide information on adhesion distribution on the cell or within ECM. Fluorescent microscopy, on the other hand, can be used to better appreciate adhesion distribution, yet this technique can neither provide similar mechanical information nor easily resolve structures smaller than hundreds of nm without complex image filtering, such as using point-spread functions. As has been previously well documented, the distribution and size of these adhesive sites is much smaller than this resolution limit (Hay 1991, Reilly and Engler 2009), so their detection will require a combination of these techniques.

To detect and determine the localization of potential submicron-sized adhesive regions, here we propose exploiting the high lateral resolution of a piezo-controlled microscope stage with force spectroscopy for a technique we have termed force spectroscopy mapping (FSM). This technique combines force sensitivity and high lateral resolution to create 'maps' of surfaces that indicate how adhesion forces change as a function of position. Using an atomic force microscope (AFM) tip, our technique is limited only in lateral resolution by the diameter of our tip, which is typically 20 nm, and in force resolution by thermal oscillations of the tip. Moreover, coupling this technique with an AFM-mounted fluorescent microscope enables dual fluorescence and FSM imaging, which makes it possible to align features that are large enough to be detectable using both imaging techniques, e.g. micron-sized features made via microcontact printing.

2. Methods

All materials were obtained from Sigma (St Louis, MO), unless otherwise noted. All values are shown as average ± standard deviation unless otherwise noted.

2.1. Preparation of polyacrylamide gels

Polyacrylamide (PA) solution was prepared using a mixture of 0.1% w/v bis-acrylamide crosslinker and 10% w/v of acrylamide monomer (C_3H_5NO) providing the elasticity of ~11 kPa (Engler *et al* 2007). To initiate the polymerization, 1/100 volume of 10% ammonium persulfate and 1/1000 volume of N, N, N', N'-tetramethylethylenediamine were added to the PA solution. 25 μl of the solution was dropped on a chlorosilanized coverslip to ensure easy detachment and a flat and uniform gel surface once polymerized. A glutaraldehyde-treated aminosilanized coverslip 25 mm in diameter was placed on the top. Following polymerization, PA hydrogel bound covalently to the top circular coverslip. The hydrogel-coated coverslips were placed in a six-well plate filled with dH_2O and kept in 4 °C until the protein of interest was immobilized.

2.2. Microcontact printing (μCP)

To immobilize protein on the PA gel, a microcontact printing technique was applied as modified from Tien and Chen (Tien and Chen 2002). Briefly, a polydimethylsiloxane (PDMS) stamp was created from a silicon wafer master containing 500 nm silicon dioxide features, i.e. 5 μm × 5 μm rectangles, which was fabricated using standard photolithographic techniques (Innovative Solutions; Sofia, Bulgaria). To make the master less adhesive, it was treated with a vapor of (tridecafluoro-1,1,2,2-tetrahydrooctyl)-1-trichlorosilane (United Chemical Technologies, Bristol, PA) for 60 min. Stamps of PDMS were then made by curing Sylgard 184 (Dow-Corning) for ~1 h against the silanized silicon master. 100 μl of a 9:1 mixture of 100 μg ml^{-1} rat plasma fibronectin and 100 μg ml^{-1} FITC-conjugated fibronectin was incubated for 30 min at room temperature on the PDMS stamp surface.

Before μCP, the PA gel was treated with sulfosuccini-midyl-6-(40-azido-20-nitrophenylamino) hexanoate (sulfo-SANPAH; Pierce, Rockford, IL) to act as a crosslinker between the gel and fibronectin. The phenylazide group of sulfo-SANPAH covalently binds to polyacrylamide on photoactivation at 365 nm, leaving the sulfosuccinimidyl group to react with primary amines of fibronectin. Sulfo-SANPAH-treated PA gel was dehydrated at 60 °C for 30 min, while the stamp was incubated with the fibronectin solution. Excess fibronectin solution was removed from the stamp, which was then inverted and placed onto the dehydrated gel. Pressure was kept on the stamp for 90 s using tweezers before gently peeling the gel off. The patterned gel was then rehydrated overnight. Pattern features are shown in figure 5(B) with a grid of 5 μm × 5 μm rectangles spaced 5 μm apart. The dimension and the orientation of the pattern were examined using the fluorescence microscope before force mapping.
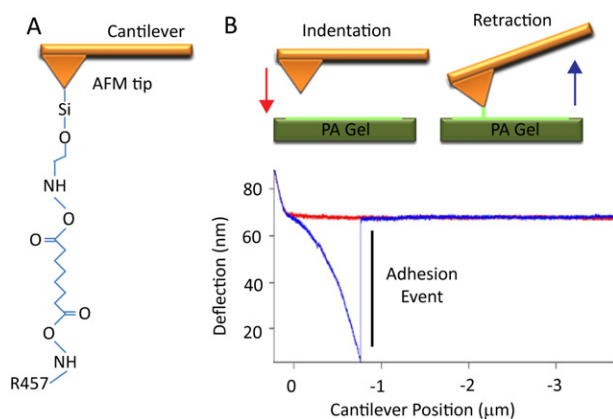
Figure 1. (A) Tip functionalization schematic depicting the attachment of the R457 antibody using the BS3 crosslinker. (B) Spectrograph (bottom) of a typical adhesion force curve containing an event of binding between the antibody and fibronectin, which has been labeled 'Adhesion Event'. This is the result from tip indentation into the material (top; red arrow), bond formation between the functionalized tip and substrate (green tether), and bond rupture upon tip retraction (top; blue arrow).

2.3. AFM cantilever functionalization

Gold-coated, pyramid-shape tips SiN cantilevers (TR400PB; Olympus; Center Valley, PA) were functionalized (figure 1(A)) with the antibody R457, rabbit polyclonal anti-rat antiserum against the amino terminal 70 kDa fragment of fibronectin (Aguirre *et al* 1994), using a previously establish method (Bonanni *et al* 2005). Briefly, the cantilevers were cleaned with chloroform and incubated with ethanolamine–HCL in dimethylsulfoxide overnight, resulting in amine group functionalization on the cantilever tips. After rinsing with phosphate-buffered saline (PBS), tips were incubated in 25 mM BS3 (bis[sulfosuccinimidyl] suberate; Pierce) for 30 min. After rinsing again, tips were then incubated in 100 μg ml^{-1} R457 for 30 min to crosslink the antibody and tip. Functionalized cantilevers were kept in the 4 °C until use.

2.4. Force spectroscopy mapping

PA gel samples were placed on an MFP-3D-BIO atomic force microscope (AFM; Asylum Research; Santa Barbara, CA) with a BioHeater Closed Fluid Cell. Using custom software written in Igor Pro (Wavemetrics; Portland, OR), samples were placed in PBS and indented in a regular array of points with a resolution of 400 data points per μm^2 using a SiN cantilever with a spring constant $k_{sp} = 20$ pN nm^{-1}, a scan area of 100–400 μm^2 as indicated, and an indentation velocity of 5 μm s^{-1} unless otherwise noted ($\sim$100 nN s^{-1}). Indentation into the gel was set not to exceed 10 nm in all cases. To promote binding of the antibody-coated cantilever and the fibronectin-coated substrate, a dwell time of 3 s was added between tip indentation (figure 1(B); red) and retraction cycles (figure 1(B); blue). Knowing the resulting deflection and cantilever spring constant and assuming Hookean behavior for the cantilever, deflection versus cantilever position data could be converted into force–indentation spectrographs (Rotsch *et al*

1999). Data were then analyzed to determine the maximum adhesive force, i.e. the greatest difference between the retraction curve and baseline. Using each force measurement's *x*- and *y*-position, data were then plotted on a map of the surface and interpolated to generate a force spectroscopy map. The maps shown in figures 2, 4, and 6 are averages of at least five maps of the identical surface.

3. Results

3.1. Mapping adhesion forces using force spectroscopy

An atomic force microscope (AFM) tip, functionalized as indicated in figure 1(A), was indented into a compliant polyacrylamide (PA) hydrogel to allow the amino terminal 70 kDa fragment of fibronectin to bind to the R457 antibody (Aguirre *et al* 1994). As shown in the force spectrogram in figure 1(B), upon retraction of the tip from the hydrogel surface, a large adhesive force was observed, which was created by the deflection of the AFM tip as it was retracted from the surface. Low force, charge-based interactions between the tip and unfunctionalized gel do not significantly bend the tip but rather result in forces driven by thermal fluctuations in the tip (not shown). Force spectrograms from functionalized surfaces contain up to three adhesive events (labeled in figure 1(B)), though the final, largest event corresponds to the force for breaking the bond between the R457 antibody and fibronectin. This positive quantity is what we call the 'adhesion force', between the tip and the substrate.

To confirm the presence of fibronectin prior to indentation, FITC-labeled fibronectin was crosslinked to the substrate (figure 2, right). Force spectroscopy maps averaged from five spectrographs of the same 20 μm × 20 μm region (figure 2, left) show the distribution of the adhesion forces in the area of the scan. The average adhesion force for unfunctionalized samples was 60.25 ± 27.18 pN, and was chosen over bovine serum albumin (BSA) coating (data not shown) to minimize charge-based interactions, which induced only ±3 nm tip deflection. It is important to note that a few adhesive interactions for the unfunctionalized substrate result in forces larger than 2.0 nN, e.g. the dark blue spot on figure 2(A), left, due to our effort to minimize non-specific binding via averaging of multiple spectrography and probed regions. On the other hand, the specific interaction between the tip and surface when functionalized with fibronectin was 360.75 ± 163.30 pN (figure 3(A)), almost sixfold larger than the unfunctionalized substrate one. Though there is a relatively uniform distribution of the fluorescent signal, the percentage deviation for the functionalized sample, i.e. the 'roughness' of the surface, is $\sim$45%. This may be indicative of the small contact area, determined by the Hertz model to be <1 nm^2 (Rotsch *et al* 1999), which ensured that a minimal number of bonds formed during an adhesion event.

3.2. Loading rate and temperature effects

The strength of bonding between the cells and their substrate likely behaves in a similar manner to that of the bonds formed between receptor-coated AFM tips and their immobilized

Unfunctionalized

Fibronectin-functionalized
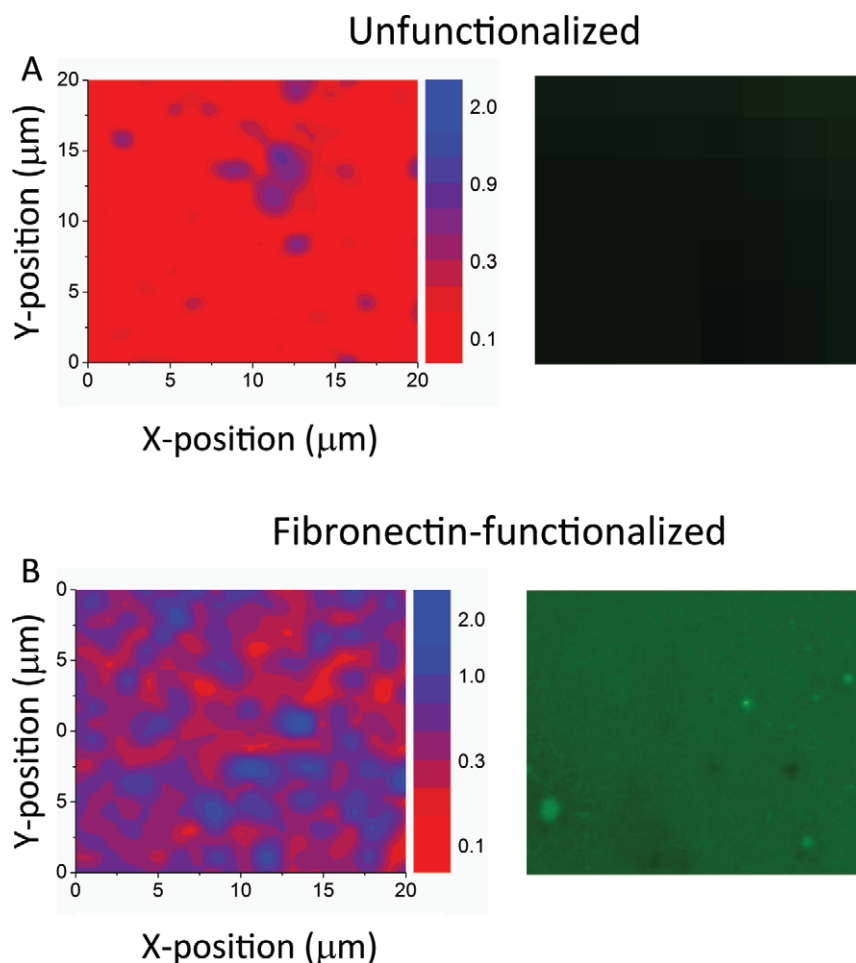
Figure 2. The average force maps (left) and fluorescent images (right) of the unfunctionalized and fibronectin-functionalized PA gel for a 20 μm × 20 μm region, respectively. The color scale is shown in nN.

ligand, as has been previously shown. (Merkel *et al* 1999, Shi and Boettiger 2003). For such systems, the bonds that form have 'catch' characteristics, as bond strength can be influenced by the rate of force application, i.e. how quickly the receptor–ligand bond is stressed. To ensure that this mapping technique is probing the adhesive domains of this bond type and not a non-specific interaction between fibronectin and the antibody, the loading rate dependences of the bonds formed during force spectroscopy mapping were tested using rates that varied from 2 to 200 nN s^{-1} (figure 3(B)). For the unfunctionalized gel, the average adhesion forces did not vary dramatically, as expected for low force, charge-based interactions. However for the fibronectin-functionalized gel, the average adhesion force increased from fourfold, with a dramatic increase above 20 nN s^{-1} indicative of 'catch bond' characteristics (Merkel *et al* 1999).

Cell–substrate adhesion is typically maintained at physiological temperature, and the lifetime and strength of these bonds would appear to be optimized for this purpose. Regardless of the temperature, unfunctionalized gels did not support measurable adhesion (data not shown) while adhesion maps of fibronectin-functionalized gels showed that these gels supported sufficient adhesion both at room temperature and at physiological temperature, i.e. 25 and 37 °C respectively

(figure 4). At supraphysiological temperature (60 °C), the adhesion force was statistically similar to that for unfunctionalized gels.

3.3. The adhesion map of a microcontact printed (μCP) fibronectin pattern

A distinct advantage of FSM over fluorescent microscopy techniques or convention force spectroscopy is that it can provide both spatial information about the distribution of adhesive ligands on a substrate and mechanical information about its capacity to bond to ligands. As is often the case, ligands are not uniformly coated on a material or distributed in a three-dimensional matrix (Reilly and Engler 2009). To demonstrate the use of FSM to detect these spatial differences in adhesive ligand distribution, a μCP technique (Tien and Chen 2002) was employed to pattern FITC-conjugated fibronectin on a gel (figure 5(A)), resulting in 5 μm × 5 μm fibronectin features (fluorescently shown in figure 5(B)). The AFM tip was aligned with these surface features and systematically probed (figure 6(A); dashed red trapezoid) to generate a corresponding adhesion force map (figure 6(B)) where the dashed green squares highlight the adhesive, FITC-conjugated fibronectin pattern. Note
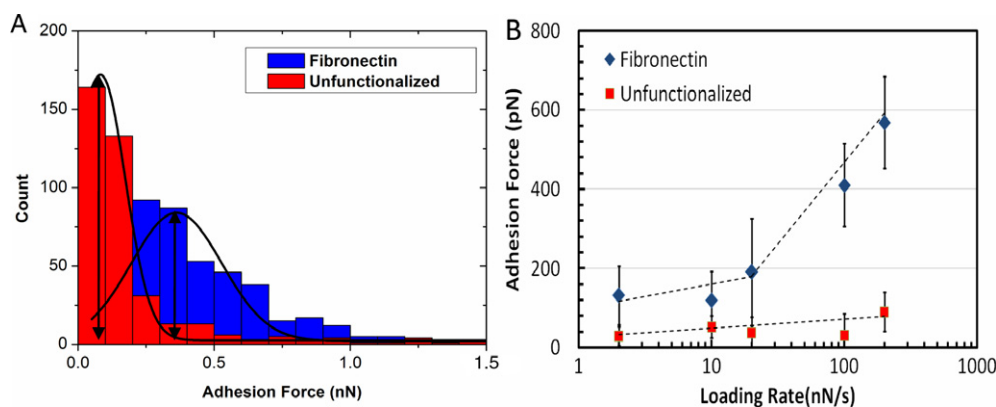
Figure 3. (A) Histogram of unfunctionalized (red) and fibronectin-functionalized (blue) PA gel fitted with a Gaussian distribution ($n = 400$). (B) Average adhesion force plotted against loading rates for the unfunctionalized (red square symbol) and fibronectin-functionalized (blue diamond symbol) PA gel. Error bars indicate the standard deviation. $n = 400$ forcespectrograms/rate. Data fits were performed with straight lines, though for the functionalized substrate, two separate lines were used to indicate different loading rate dependences.
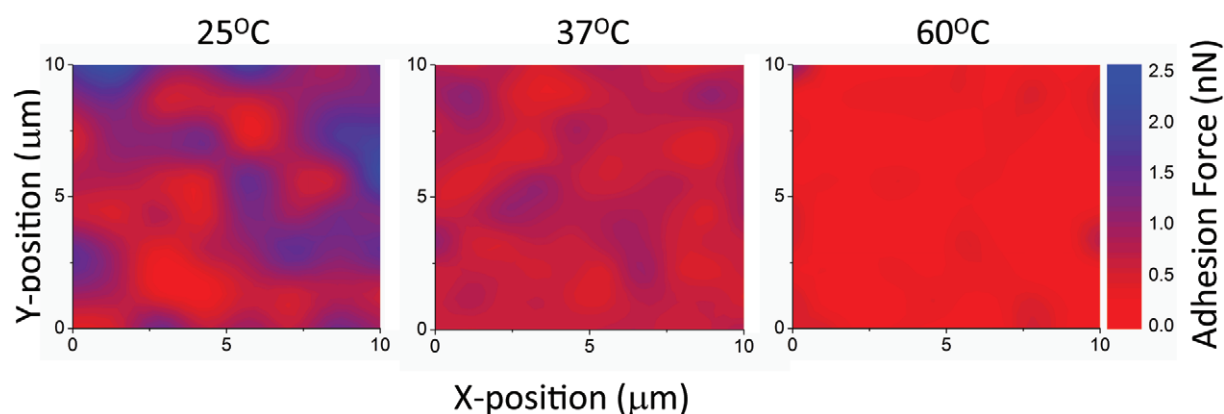
Figure 4. The average adhesion force maps from 10 force maps of the fibronectin-functionalized PA gel on a 10 μm $\times$ 10 μm region at the temperatures of 25, 37, and 60 °C, left to right respectively.

that no significant detachment of fibronectin was observed during FSM probing (supplemental figure 1 available at stacks.iop.org/JPhysCM/22/194102/mmedia); thus any change in the average force map was not a result of ligand loss. Adhesion forces of the fibronectin features were similar to those found for uniformly functionalized substrates (figure 2(B)), though the unfunctionalized regions had forces that were twofold higher than those of the uniformly unfunctionalized substrate (figure 2(A)) and perhaps indicate regions where low levels of fibronectin exist but which are not detectable by light microscopy. Despite the smaller difference in force magnitude, it does appear that FSM could be used to detect features resembling squares, as Student t-tests of forces from patterned and unpatterned regions were significantly different ($p < 10^{-4}$).

4. Discussion

4.1. Materials with a distribution of 'sticky' patches

Our comparison here between a patterned, protein-functionalized material and the material's non-adhesive, unfunctionalized surface emphasizes our ability to recognize patterns at sufficient resolution that have not previously seen (Dague *et al* 2007, Dupres *et al* 2007, Gunning *et al* 2008, Verbelen and Dufrene 2009); it should be noted, however, that our antibody–fibronectin interaction could withstand upwards of 500 pN of force versus low forces from the unfunctionalized surface (figure 3(A)). Compared to the interaction previously mapped between bacteria hemagglutinin and heparin (Dupres *et al* 2007) and those measured for streptavidin–biotin (Yuan *et al* 2000), mycobacterial protein–fibronectin (Verbelen and Dufrene 2009), and normal integrin–ECM bonds (Jiang *et al* 2003, Li *et al* 2003, Sun *et al* 2005), the forces observed here are at least an order of magnitude higher, which may account for improved pattern recognition (Muller *et al* 2009). Although the higher magnitude and the presence of single unbinding peaks does not rule out the formation of parallel bonds to achieve higher rupture forces, it further enhances our detection capabilities and emphasizes the differences in forces seen in the patterned substrate, e.g. statistically different force distributions in the functionalized and unfunctionalized regions ($p < 10^{-4}$) typical of the sixfold force difference between the two substrates (figure 2). That said, spectrograms did not
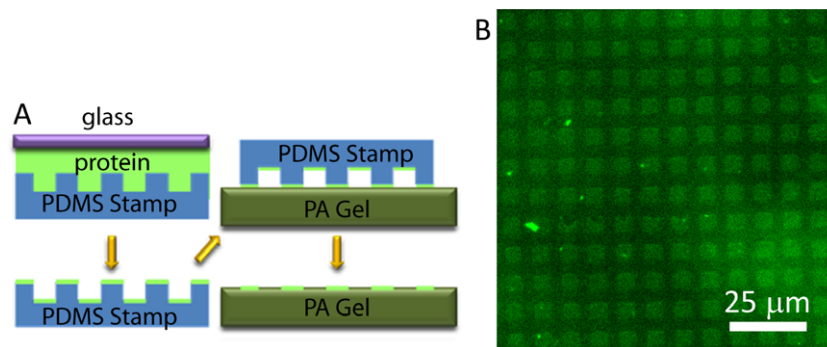
Figure 5. (A) Schematic of the technique of microcontact printing (μCP) on the sulfo-SANPAN initiated PA gel. (B) A fluorescent image of the 5 μm $\times$ 5 μm fibronectin–FITC patterned PA gel. The scale bar is 25 μm.
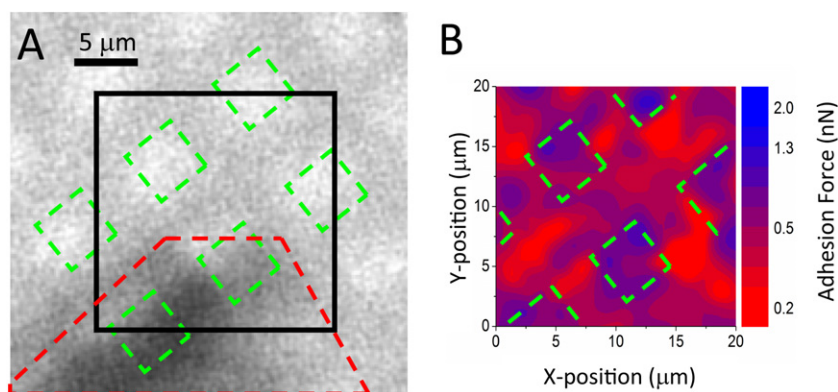
Figure 6. (A) Schematic of the pattern beneath the AFM cantilever tip (red dashed trapezoid) indicating the AFM scanning area (black solid rectangle) and fibronectin-functionalized squares (green dashed rectangles). Note that the dark regions in the fluorescent image are due to the cantilever positioned above the substrate. (B) Force spectroscopy map of the substrate using the region shown in part (A) outlined by the solid rectangle line. The average of eight force maps (with a resolution of 1 scan μm^{-2}) was overlaid with the 5 μm $\times$ 5 μm fibronectin-functionalized pattern (green dashed lines) from part (A).

indicate tandem events (Law *et al* 2003), and given typical antibody affinities for R457 (Aguirre *et al* 1994), this may well represent single antibody–fibronectin bonds.

Most natural and synthetic materials do not have a repeating pattern of adhesive regions; instead of a regular array of adhesive islands presented by μCP, they have a random distribution of ligands. For example, the R–G–D domain of fibronectin is only seen for cells when fibronectin is unwound and assembled into a fiber in which the 10th type 3 domain is accessible (Mao and Schwarzbauer 2005, Ruoslahti and Pierschbacher 1987). Moreover after cells adhere to ECM, they often actively remodel their matrix, and this further complicates the characterization of cell adhesion site distribution, especially that of those submicron sites which escape detection by conventional microscopy. Yet for matrix with an unknown distribution of 'sticky' patches or to investigate cells (Gunning *et al* 2008), our specific method of FSM can provide improved characterization, determining the distribution of adhesion sites with high lateral resolution of 20 nm (figure 6) as well as being sensitive to small changes in the strength of adhesion by using flexible cantilevers, $k_{sp} \sim 20$ pN nm^{-1} (figures 3, 4). However, there may be significant complications provided by the fibrillar structure

of these matrices (Hay 1991, Mao and Schwarzbauer 2005) and the presence of cells versus a smooth functionalized hydrogel surface. Non-cell-adhesive regions of fibronectin may have higher non-specific adhesion forces compared with the unfunctionalized substrate here, making the detection of adhesive features within the matrix less accurate, as with BSA coating. Using species-specific antibodies could overcome such a limitation; force spectrograms using a human-specific fibrinogen antibody could detect fivefold force differences between human fibrinogen and BSA (Agnihotri and Siedlecki 2005), compared to our pan-fibronectin antibody recognizing the 70 kD amino terminal end of most fibronectin species (Aguirre *et al* 1994).

4.2. Exploiting dynamic responses and specificity of the antibody–fibronectin bond for FSM

As for other biological receptor–ligand interactions, e.g. streptavidin–biotin ones (Merkel *et al* 1999), fibronectin does not have the ideal, single energy barrier, and thus as the loading rate of the tip increases, the rupture force increase is non-linear (Frisbie *et al* 1994). Thus this transition in rupture force, which was observed at 20 nN s^{-1} here (figure 3(B)), is the result of a change in the inner activation barrier of the complex

Table 1. Evolution of the force spectroscopy mapping technique. A subset of the relevant results for adhesion-based spectroscopy mapping summarized in table 1 show our ability to measure a transition state in full length fibronectin binding, which previously has not been observed. Using higher loading rates, we can then detect microsized feature patterns with the high resolution of other studies but using fibronectin and imaging with much higher fidelity.

Measurement	Adhesion	Rupture force	Lateral map resolution	Patterned feature recognition	Citation
Force spectroscopy	Avidin–biotin	Multiples of 160 ± 20 pN	—	—	Florin *et al* (1994)
	Streptavidin–biotin	Force transition state at 1 nN s^{-1}	—	—	Yuan *et al* (2000)
	Fibronectin–*S. epidermidis*	No force transition state, 100s of pN rupture force	—	—	Bustanji *et al* (2003)
	Fibronectin–$\alpha5\beta1$ integrin	Force transition state at 10 nN s^{-1}	—	—	Li *et al* (2003)
	Fibronectin–heparin	No force transition state, 100s of pN rupture force	—	—	Mitchell *et al* (2007)
Force spectroscopy mapping	Patterned carboxyl and methyl groups	8.7 ± 3.2 nN for carboxyl groups	25 μm^{-2}	Yes, tens of micron-sized features	Frisbie *et al* (1994)
	Streptavidin–biotin	$\sim$1 nN	$\sim$10 μm^{-2}	Yes, micron-sized features	Ludwig *et al* (1997)
	Hemagglutinin–heparin on mycobacteria	50 ± 23 pN and 117 ± 18 pN for single and double rupture	400 μm^{-2}	Not able to determine	Dupres *et al* (2007)
	Hydrophobic tip interaction with *Aspergillus fumigatus*	3.0 ± 0.4 nN	400 μm^{-2}	Yes, micron-sized features	Dague *et al* (2007)
	Agglutinin–epidermal growth factor receptor in Caco-2 cells	Modal value of 125 pN	<1 μm^{-2}	Yes, tens of micron-sized features	Gunning *et al* (2008)
	Mycobacteria–fibronectin associated proteins	52 ± 19 pN	400 μm^{-2}	Not able to determine	Verbelen and Dufrene (2009)
	Fibronectin–R457 antibody	Force transition state at 20 nN s^{-1} and maximum rupture force of 2.44 nN	400 μm^{-2}	Yes, micron-sized features where $p < 10^{-4}$	Current study

(Li *et al* 2003), which also occurs in other complex bonds such as mycobacterial protein–fibronectin bonds (Verbelen and Dufrene 2009) and integrin–fibronectin bonds (Li *et al* 2003). In other words when the fibronectin–antibody bond forms, it induces a conformational change in the proteins which stabilizes their ability to resist increasing force when applied faster. Formally, this behavior is predicted by the Bell model of adhesion (Bell 1978, Evans and Ritchie 1997), where the antibody–fibronectin bond illustrates a catch bond. The strong non-covalent interaction between the antibody and its 70 kD target Aguirre *et al* (1994) likely confers a conformational change similar to that for fibronectin–integrin binding (Li *et al*

2003). Thus we are able to produce up to a sixfold difference in adhesion force to aid in our ability to recognize surface features. It is important to note that this transition state is intrinsic to the specific interaction; while we previously noted the fibronectin interaction transitions at 20 nN s^{-1} (Li *et al* 2003), the streptavidin–biotin transition occurs at 1 nN s^{-1} (Yuan *et al* 2000). Thus feature detection with other molecules may be easier, as is the case with lower transition bonds such as streptavidin–biotin ones, or more difficult, with bonds whose transition state is higher. Fortunately for the detection of cell adhesion molecules on a material, many cell–ECM (Li *et al* 2003, Muller *et al* 2009) and specific cell–cell bonds,

e.g. E-cadherin (Panorchan *et al* 2006) but not N-cadherin (Shi and Boettiger 2003), have bond transition states such that sufficient loading rates can produce maximal differences in bond forces between functionalized and unfunctionalized regions of the substrate. Continually increasing the loading rate to further exploit this difference appears plausible; however the Bell model (Bell 1978, Evans and Ritchie 1997) indicates that there is a limit to the loading rate due to the surrounding solution's viscous damping (Siria *et al* 2009). The transition state for fibronectin amplifies our ability to recognize patterns at high resolution and with high fidelity, unlike previous spectroscopy or pattern mapping studies, as summarized in table 1. On the other hand, many simple chemical bonds between functional groups (Frisbie *et al* 1994) or with alkanethiol bonds (Dague *et al* 2007) lack this transition and would not be as easily mapped.

Bonds have specific lifetimes and affinities, and to increase detectability, the antibody–fibronectin bond was chosen. The duration of the contact between the tip and sample surface has also been used to increase adhesive interactions (Lü *et al* 2006). Here the contact duration was fixed at 3 s, resulting in 74% of the binding events producing forces twofold higher than the average non-specific binding force. However, Lü and co-workers found that contact time greater than 500 ms does not shift the peak force (Lü *et al* 2006), and while force saturation is likely dependent on the particular bond, it is nonetheless indicated that contact time is not as critical a factor with high affinity bonds as other parameters, e.g. loading rate. Minimizing contact time should decrease scan time while not requiring sacrifice of mapping resolution.

5. Conclusion

High resolution FSM using loading rates above the receptor–ligand transition point as presented here is a useful technique for accurately determining the spatial variation of material components within a substrate where such variation is not known. Moreover, coupling FSM with conventional fluorescence microscopy can further enhance our understanding of complex materials and how cellular responses are dictated by the arrangement of adhesive ligands.

Acknowledgments

References

Agnihotri A and Siedlecki C A 2005 Adhesion mode atomic force microscopy study of dual component protein films *Ultramicroscopy* **102** 257–68

Aguirre K M, McCormick R J and Schwarzbauer J E 1994 Fibronectin self-association is mediated by complementary sites within the amino-terminal one-third of the molecule *J. Biol. Chem.* **269** 27863–8

Bell G I 1978 Models for the specific adhesion of cells to cells *Science* **200** 618–27

Bonanni B, Kamruzzahan A S M, Bizzarri A R, Rankl C, Gruber H J, Hinterdorfer P and Cannistraro S 2005 Single molecule recognition between cytochrome C 551 and gold-immobilized azurin by force spectroscopy *Biophys. J.* **89** 2783–91

Bustanji Y, Arciola C R, Conti M, Mandello E, Montanaro L and Samori B 2003 Dynamics of the interaction between a fibronectin molecule and a living bacterium under mechanical force *Proc. Natl Acad. Sci. USA* **100** 13292–7

Chien S, Li S, Shiu Y T and Li Y S 2005 Molecular basis of mechanical modulation of endothelial cell migration *Front. Biosci.* **10** 1985–2000

Chiquet M, Gelman L, Lutz R and Maier S 2009 From mechanotransduction to extracellular matrix gene expression in fibroblasts *Biochim. Biophys. Acta (BBA)—Mol. Cell Res.* **1793** 911–20

Dague E, Alsteens D, Latge J P, Verbelen C, Raze D, Baulard A R and Dufrene Y F 2007 Chemical force microscopy of single live cells *Nano Lett.* **7** 3026–30

Dufrene Y F and Hinterdorfer P 2008 Recent progress in AFM molecular recognition studies *Pflugers Arch.* **456** 237–45

Dupres V, Verbelen C and Dufrene Y F 2007 Probing molecular recognition sites on biosurfaces using AFM *Biomaterials* **28** 2393–402

Engler A J, Chan M, Boettiger D and Schwarzbauer J E 2009a A novel mode of cell detachment from fibrillar fibronectin matrix under shear *J. Cell Sci.* **122** 1647–53

Engler A J, Humbert P O, Wehrle-Haller B and Weaver V M 2009b Multiscale modeling of form and function *Science* **324** 208–12

Engler A J, Rehfeldt F, Sen S, Discher D E and Wang Y L 2007 Microtissue elasticity: measurements by atomic force microscopy and its influence on cell differentiation *Methods in Cell Biology* vol 83 (New York: Academic) pp 521–45

Evans E and Ritchie K 1997 Dynamic strength of molecular adhesion bonds *Biophys. J.* **72** 1541–55

Florin E L, Moy V T and Gaub H E 1994 Adhesion forces between individual ligand–receptor pairs *Science* **264** 415–7

Friedland J C, Lee M H and Boettiger D 2009 Mechanically activated integrin switch controls $\alpha 5\beta 1$ function *Science* **323** 642–4

Frisbie C D, Rozsnyai L F, Noy A, Wrighton M S and Lieber C M 1994 Functional group imaging by chemical force microscopy *Science* **265** 2071–4

Gallant N D, Michael K E and Garcia A J 2005 Cell adhesion strengthening: contributions of adhesive area, integrin binding, and focal adhesion assembly *Mol. Biol. Cell* **16** 4329–40

Griffin M A, Engler A J, Barber T A, Healy K E, Sweeney H L and Discher D E 2004 Patterning, prestress, and peeling dynamics of myocytes *Biophys. J.* **86** 1209–22

Gunning A P, Chambers S, Pin C, Man A L, Morris V J and Nicoletti C 2008 Mapping specific adhesive interactions on living human intestinal epithelial cells with atomic force microscopy *FASEB J.* **22** 2331–9

Hay E D 1991 *Cell Biology of Extracellular Matrix* (New York: Plenum) p 468

Hinz B and Gabbiani G 2003 Cell–matrix and cell–cell contacts of myofibroblasts: role in connective tissue remodeling *Thromb. Haemost.* **90** 993–1002

Ingber D E 2008 Can cancer be reversed by engineering the tumor microenvironment? *Semin. Cancer Biol.* **18** 356–64

Jiang G, Giannone G, Critchley D R, Fukumoto E and Sheetz M P 2003 Two-piconewton slip bond between fibronectin and the cytoskeleton depends on talin *Nature* **424** 334–7

Kumar S and Weaver V M 2009 Mechanics, malignancy, and metastasis: the force journey of a tumor cell *Cancer Metastasis Rev.* **28** 113–27

Law R, Carl P, Harper S, Dalhaimer P, Speicher D W and Discher D E 2003 Cooperativity in forced unfolding of tandem spectrin repeats *Biophys. J.* **84** 533–44

Li F, Redick S D, Erickson H P and Moy V T 2003 Force measurements of the $\alpha5\beta1$ integrin fibronectin interaction *Biophys. J.* **84** 1252–62

Li S, Guan J-L and Chien S 2005 Biochemistry and biomechanics of cell motility *Annu. Rev. Biomed. Eng.* **7** 105–50

Ludwig M, Dettmann W and Gaub H E 1997 Atomic force microscope imaging contrast based on molecular recognition *Biophys. J.* **72** 445–8

Ludwig T, Kirmse R, Poole K and Schwarz U 2008 Probing cellular microenvironments and tissue remodeling by atomic force microscopy *Pflügers Arch. Eur. J. Physiol.* **456** 29–49

Lü S, Ye Z, Zhu C and Long M 2006 Quantifying the effects of contact duration, loading rate, and approach velocity on P-selectin–PSGL-1 interactions using AFM *Polymer* **47** 2539–47

Mao Y and Schwarzbauer J E 2005 Fibronectin fibrillogenesis, a cell-mediated matrix assembly process *Matrix Biol.* **24** 389–99

Merkel R, Nassoy P, Leung A, Ritchie K and Evans E 1999 Energy landscapes of receptor–ligand bonds explored with dynamic force spectroscopy *Nature* **397** 50–3

Mitchell G, Lamontagne C A, Lebel R, Grandbois M and Malouin F 2007 Single-molecule dynamic force spectroscopy of the fibronectin–heparin interaction *Biochem. Biophys. Res. Commun.* **364** 595–600

Muller D J, Helenius J, Alsteens D and Dufrene Y F 2009 Force probing surfaces of living cells to molecular resolution *Nat. Chem. Biol.* **5** 383–90

Panorchan P, George J P and Wirtz D 2006 Probing intercellular interactions between vascular endothelial cadherin pairs at single-molecule resolution and in living cells *J. Mol. Biol.* **358** 665–74

Puklin-Faucher E and Sheetz M P 2009 The mechanical integrin cycle *J. Cell Sci.* **122** 179–86

Reilly G C and Engler A J 2009 Intrinsic extracellular matrix properties regulate stem cell differentiation *J. Biomech.* **43** 55–62

Rotsch C, Jacobson K and Radmacher M 1999 Dimensional and mechanical dynamics of active and stable edges in motile fibroblasts investigated by using atomic force microscopy *Proc. Natl Acad. Sci. USA* **96** 921–6

Ruoslahti E and Pierschbacher M D 1987 New perspectives in cell adhesion: RGD and integrins *Science* **238** 491–7

Shao J Y, Xu G and Guo P 2004 Quantifying cell-adhesion strength with micropipette manipulation: principle and application *Front. Biosci.* **9** 2183–91

Sharma R I, Shreiber D I and Moghe P V 2008 Nanoscale variation of bioadhesive substrates as a tool for engineering of cell matrix assembly *Tissue Eng.* A **14** 1237–50

Shi Q and Boettiger D 2003 A novel mode for integrin-mediated signaling: tethering is required for phosphorylation of FAK Y397 *Mol. Biol. Cell* **14** 4306–15

Siria A, Drezet A, Marchi F, Comin F, Huant S and Chevrier J 2009 Viscous cavity damping of a microlever in a simple fluid *Phys. Rev. Lett.* **102** 254503

Sun Z, Martinez-Lemus L A, Trache A, Trzeciakowski J P, Davis G E, Pohl U and Meininger G A 2005 Mechanical properties of the interaction between fibronectin and $\alpha5\beta1$-integrin on vascular smooth muscle cells studied using atomic force microscopy *Am. J. Physiol. Heart Circ. Physiol.* **289** H2526–35

Tien J and Chen C S 2002 Culture environments: microarrays *Methods of Tissue Engineering* (New York: Academic) pp 113–20

Verbelen C and Dufrene Y F 2009 Direct measurement of mycobacterium–fibronectin interactions *Integr. Biol.* **1** 296–300

Yuan C, Chen A, Kolb P and Moy V T 2000 Energy landscape of streptavidin–biotin complexes measured by atomic force microscopy *Biochemistry* **39** 10219–23